

EXTRAPOLATING LARGE MODELS FROM THE SMALL: OPTIMAL LEARNING OF SCALING LAWS

005 **Anonymous authors**

006 Paper under double-blind review

ABSTRACT

011 As large language models (LLMs) continue to scale to billions of parameters,
 012 training them becomes increasingly expensive, making it infeasible to exhaustively
 013 explore the vast design space including model architectures, parameter
 014 sizes, and compute budgets. Scaling laws have therefore emerged as an essential
 015 tool for predicting the performance of larger models by extrapolating from smaller
 016 ones, enabling practitioners to make informed design choices without full-scale
 017 training. However, existing approaches lack formal guarantees on the predicted
 018 results and overlook the out-of-distribution nature of such extrapolation, leading
 019 to instability and unreliable predictions. We address these challenges with three
 020 key contributions. First, we introduce *Equivalent Sample Size* (ESS), a principled
 021 and interpretable metric that quantifies prediction uncertainty by translating
 022 it into the number of test samples required for direct, in-distribution evaluation.
 023 Second, we analyze how extrapolation amplifies prediction variance and develop
 024 an efficient algorithm that optimally allocates smaller-model evaluations to maxi-
 025 mize ESS under compute budgets. Third, experiments on both simulated and real
 026 datasets show that ESS and our algorithm guide the design of scaling-law learning,
 027 cut evaluation cost, and deliver reliable LLM performance predictions.

1 INTRODUCTION

031 The development of large language models (LLMs) has been driven by the intuition that scaling up
 032 model size, data volume, and compute generally leads to better performance (Kaplan et al., 2020).
 033 However, pre-training modern LLMs requires immense computational resources, often costing mil-
 034 lions of dollars and weeks of training time across thousands of GPUs. As a result, blindly increasing
 035 one dimension such as model size, has become increasingly inefficient and impractical. There is a
 036 growing demand for principled tools that can guide pre-training decisions before these expensive
 037 investments are made Touvron et al. (2023); Bi et al. (2024); Choshen et al. (2024).

038 A promising direction is the use of scaling laws, which posit power-law relationships between model
 039 performance and key design variables such as model size and dataset size (Rosenfeld et al., 2019;
 040 Kaplan et al., 2020; Hoffmann et al., 2022). These empirical laws enable predicting the performance
 041 of a target large model by extrapolating from the observed performance of smaller models – a frame-
 042 work that we referred to as *scaling prediction* through the paper. Scaling prediction can therefore
 043 help prioritize architectures, optimize resource allocation, and reduce experimentation cost. Recent
 044 studies have demonstrated that such predictions can be surprisingly accurate in practice (Ruan et al.,
 045 2025; Chen et al., 2024; Zhang et al., 2024; Wu & Tang, 2024; Xu et al., 2025), reinforcing the value
 046 of scaling laws as an essential tool for efficient LLM development.

047 While promising, scaling prediction faces two fundamental challenges that remain underexplored.
 048 First, there is no guarantee on the accuracy or confidence of the predicted results. Existing methods
 049 primarily employ regression fitting with small-scale model quantities and extrapolate performances
 050 to large models. However, scaling prediction is intrinsically an *out-of-distribution* (OOD) prediction
 051 problem Liu et al. (2021); Ye et al. (2021) (i.e., using data from small-scale regime to predict perfor-
 052 mance in large-scale regimes) whose optimal learning requires very careful treatment. Second, as
 053 we found, existing approaches of simply running regression on random samples suffer from inher-
 ent instability due to its nature of extrapolation from small models to the large. Due to the test with

054 OOD samples, small variations or noise in the observed data can lead to disproportionately large
 055 uncertainty in the predictions (Hendrycks et al., 2021; Liu et al., 2021).
 056

057 In this work, we make three contributions to address these challenges. First, we introduce a metric
 058 coined *Equivalent Sample Size* (ESS) to quantify the quality of scaling prediction. ESS provides an
 059 intuitive interpretation: it represents how many test examples would have been required via direct,
 060 In-Distribution (ID) evaluation to achieve the same accuracy and confidence as that of the scaling
 061 prediction. This unified quantification allows practitioners to compare prediction quality across
 062 different experimental setups using different model sizes. Second, we conduct a systematic study of the
 063 scaling prediction uncertainty induced by extrapolation and solve for the optimal design of the sam-
 064 ple regime (e.g., model sizes) that achieves the maximum ESS. Specifically, under computational
 065 budget constraints, we develop a polynomial-time algorithm to determine which (smaller) model
 066 sizes to evaluate to minimize prediction uncertainty, thereby maximizing ESS. This design ensures
 067 that limited evaluation resources are used most effectively, enabling practitioners to decide whether
 068 training additional small models is worthwhile to improve prediction quality. Third, we illustrate the
 069 use of ESS and our algorithm by predicting model emergent capabilities. We find that using only
 070 three models from the OPT family is sufficient to produce a prediction on a large target model with
 071 accuracy and ESS comparable to that of using all seven available small models, leading to a sig-
 072 nificant reduction in the compute cost. The ESS also reflects the prediction quality, thus delivering
 073 reliable LLM performance predictions.
 074

075 Taken together, these contributions offer a principled foundation for predictive evaluation of LLMs
 076 via scaling prediction. By introducing ESS as a measure of prediction quality and developing algo-
 077 rithms for optimal evaluation design, *our framework leads to both more efficient scaling prediction*
 078 *via optimized sample choice and more reliable predictions that are crucial for real-world deploy-*
 079 *ment*. We hope this framework will encourage both researchers and practitioners to *rethink scaling*
 080 *law not as a passive learning task but as a strategic resource allocation problem* that can be opti-
 081 *mized to balance accuracy, cost, and confidence.*
 082

083 The rest of this paper is organized as follows. Section 2 reviews the related literature and Section 3
 084 formulates the problem. Section 4 introduces ESS for uncertainty quantification. Section 5 reveals
 085 that extrapolation inherently induces a high variance of scaling prediction, whiles Section 6 proposes
 086 an algorithm to find the optimal design for fitting the scaling law. Section 7 includes experiment
 087 results. Conclusion and further discussion are included in Section 8.
 088

089 2 RELATED WORK

090 Scaling laws have emerged as a powerful tool for understanding and predicting the behavior of
 091 LLMs. They reveal a consistent power-law relationship between an LLM’s pre-training loss or
 092 downstream-task performance and its design factors, particularly compute measures such as training
 093 FLOPs, dataset size, and model parameters (Cortes et al., 1993; Kaplan et al., 2020; Brown et al.,
 094 2020; Hoffmann et al., 2022; Zhai et al., 2022; Bahri et al., 2024; Gadre et al., 2024). Early work
 095 establishes these patterns empirically, e.g., Rosenfeld et al. (2019); Kaplan et al. (2020) shows that
 096 increasing a single dimension can lead to a smaller training loss; Hoffmann et al. (2022) proposed
 097 the Chinchilla laws to balance model size and data tokens for a fixed compute budget. More recent
 098 efforts refines these insights and explore efficient and accurate scaling laws: Alabdulmohsin et al.
 099 (2022); Caballero et al. (2022) extended beyond power-laws to more flexible functional forms; Gadre
 100 et al. (2024); Owen (2024) studied scaling on downstream tasks; Polo et al. (2024); Ruan et al.
 101 (2025) proposed scaling across model families; Choshen et al. (2024) proposed to reduce the training
 102 cost of scaling laws by choosing models sizes and tokens, while Hägele et al. (2024) advocated
 103 training models with a constant learning rate. These relationships enable researchers to forecast the
 104 performance of larger, more expensive models by leveraging empirical observations from smaller
 105 ones, thereby avoiding the prohibitive costs of direct training and evaluation.
 106

107 Existing scaling prediction methods mainly fall into two categories. The first category directly fits an
 108 end-to-end scaling law, where model performance is expressed as a power-law function of compute
 109 measures. Using observations from smaller models, the fitted curve is then extrapolated to predict
 110 the behavior of larger target models (Wu & Tang, 2024; Du et al., 2024). This approach is simple
 111 and popular due to its interpretability. However, its reliance on a single functional form (typically
 112 log-linear) makes it highly sensitive to deviations from the assumed power law.
 113

108 The second category introduces an intermediate quantity that itself scales with compute and serves
 109 as a bridge between raw resources and final performance. Examples of such intermediate quantity
 110 include pre-training loss (Chen et al., 2024) and model capability scores (Ruan et al., 2025; Polo
 111 et al., 2024). Once this intermediate variable is estimated via scaling laws, researchers then model its
 112 relationship with downstream-task accuracy using flexible predictors such as logistic regression (Xu
 113 et al., 2025; Ruan et al., 2025) or neural networks (Ye et al., 2023; Zhang et al., 2024). This two-stage
 114 approach often improves prediction accuracy, as the intermediate quantity captures generalizable
 115 patterns across tasks or model families.

116 In both approaches, the key step is extrapolating relationships fitted on small models into much
 117 larger, unseen regimes. Such extrapolation is fundamentally unstable: while small estimation errors
 118 may be tolerable in-distribution, they are amplified dramatically when extended out-of-distribution
 119 to trillion-parameter LLMs. This limitation, further analyzed in Section 5, motivates the need for
 120 systematic uncertainty quantification to make scaling prediction reliable for guiding the future LLM
 121 evaluations.

122 On the technical side, our work is related to out-of-distribution (OOD) generalization. For a com-
 123 prehensive review of OOD literature, we refer to Liu et al. (2021). Generally speaking, controlling
 124 OOD generalization is fundamentally difficult, as the test data regime is unseen in the training data.
 125 Common approaches typically assume certain relationship between OOD domain and training do-
 126 main, such as causal learning (Peters et al., 2016), invariant learning (Arjovsky et al., 2019; Zhao
 127 et al., 2019), and meta learning (Li et al., 2018). In contrast to these general OOD frameworks, scal-
 128 ing prediction owns a unique structure of extrapolating from small size to large size through power
 129 laws, hence allowing more efficient and tractable solutions.

130 3 THE SCALING PREDICTION PROBLEM AND SOURCES OF UNCERTAINTY

131 This section reviews the process of scaling prediction of model performance and demonstrates that
 132 such prediction can be highly uncertain and hence unreliable, which is overlooked in this field.

133 **Background.** Suppose we have evaluated the performance of some small models $\{f_1, \dots, f_M\}$
 134 on some tasks $\{T_1, \dots, T_K\}$, denoted as $P_{m,t}, m = 1, \dots, M, t = 1, \dots, K$. Without loss of
 135 generality, we take $P \in (0, 1)$, as any metric can be monotonically mapped to this range. Our goal
 136 is to predict the performance of a large model f^* from the same family on a task $T \in T_1, \dots, T_K$.

137 **Scaling Prediction Process.** We unify both end-to-end and intermediate scaling-law approaches
 138 as the following process. *Step 1:* Extract a critical quantity (e.g., the capability score or model
 139 performance) of training models as Y_1, \dots, Y_M . For notation simplicity, we assume that the critical
 140 quantity Y is a scalar, as the vector scenario can be analyzed in an analogous manner coordinate-
 141 wise. *Step 2:* Fit a power-law model such that

$$145 \quad Y = \alpha + \beta X + \epsilon, \quad (1)$$

146 where $X \in \mathbb{R}^p$ encodes design factors such as the logarithm of number of parameters, size of
 147 training data, and FLOPs, ϵ is Gaussian noise, and $\alpha \in \mathbb{R}, \beta \in \mathbb{R}^p$ are coefficients. Eq. (1) explains
 148 the name of scaling prediction, as one extrapolates the critical quantity Y from the small-model
 149 regime to larger X . *Step 3:* Translate the critical quantity to model performance P as follows:

$$151 \quad P = \sigma(\omega Y + b), \quad (2)$$

152 where $\sigma(\cdot)$ is a monotone link function, e.g., $\sigma(z) = 1/(1+e^{-z})$ corresponds to a logistic regression
 153 model, and ω, b are coefficients. End-to-end scaling laws are recovered by taking $\sigma(z) = z, \omega = 1$,
 154 and $b = 0$. [We discuss how our framework can be extended to broader and more realistic scenarios
 155 by relaxing assumptions such as linearity and Gaussian noise in Appendix E.3.](#)

156 *Remark 1* (Universality of the Link Function.). A nature principle in scaling prediction is that, while
 157 the critical quantity Y can be family-specific, the relationship between Y and the final performance
 158 P is largely universal across families. For example, a model’s accuracy on math problems depends
 159 mostly on its underlying math capability, regardless of architecture or training dynamics; however,
 160 the rate at which this capability grows with model size varies from family to family. Consequently,
 161 the link function in Eq. (2) can often be well-estimated by leveraging performance data from other
 model families (Chen et al., 2024; Ruan et al., 2025).

162 **Prediction Uncertainty.** The final predictor \hat{P} involves two main sources of uncertainty. The first
 163 stems from intrinsic random noise in the training data, represented by ϵ in Eq. (1). This noise arises
 164 from measurement error and randomness in the model training and lies largely beyond the
 165 practitioner’s control. Nevertheless, this source can be accurately estimated given a well-specified
 166 scaling model Eq.s (1) and (2).

167 As such, this work will focus on the second source: uncertainty introduced by extrapolation. Scaling
 168 prediction fits Eq. (1) on small models and use it to predict the performance of much larger ones.
 169 Because this applies patterns learned in a limited regime to an unseen region, even slight noise or
 170 variation in the observed data can lead to disproportionately large uncertainty in the predictions.
 171

172 To our knowledge, the uncertainty of scaling prediction has not been rigorously quantified in prior
 173 work. We therefore propose a framework to quantify and reduce the uncertainty inherent to extrapolation
 174 in the following sections.

175 **Remark 2 (Prediction Correctness v.s. Confidence).** Under the well-specified model assumption
 176 used in the main paper, high prediction confidence reliably indicates high prediction correctness.
 177 However, when the model is mis-specified, the prediction may become biased, leading to situations
 178 where the model is “confidently wrong.” In Appendix E.3, we discuss how the Equivalent Sample
 179 Size (ESS) can be used as a diagnostic tool to detect such mis-specification.

180 4 UNCERTAINTY QUANTIFICATION VIA EQUIVALENT SAMPLE SIZE

181 In this section, we address the problem of quantifying the reliability of scaling prediction. We
 182 introduce a measure called *Equivalent Sample Size (ESS)*, which has a natural interpretation from a
 183 cost-benefit perspective. Intuitively, ESS compares the information gained by fitting a scaling law
 184 on smaller models to that obtained from directly evaluating the target model on an in-distribution
 185 test dataset. It represents the number of test examples one would need in direct evaluation to achieve
 186 the same level of accuracy and confidence as the scaling prediction.

187 **Motivation of ESS.** Suppose that we want to evaluate the performance P of a target model f^* . Following
 188 Eq.s (1) and (2), scaling prediction induces a probability distribution over P . Alternatively,
 189 one could evaluate f on a test dataset. Given n samples (S_i, R_i) , $i = 1, \dots, n$, where S_i are prompts
 190 and R_i are expected responses, the empirical performance is $\hat{P}_n = n^{-1} \sum_{i=1}^n \ell(f(S_i), R_i)$, where ℓ
 191 is a loss function. For any bounded loss function ℓ , a valid $(1 - \delta)$ confidence interval for \hat{P}_n can be
 192 derived by applying Hoeffding’s inequality (Hoeffding, 1963) to the random variables $\ell(f(S_i), R_i)$.
 193 For example, under the zero-one loss, it yields $[\hat{P}_n - \epsilon_n, \hat{P}_n + \epsilon_n]$, where $\epsilon_n = \sqrt{\ln(1/\delta)/(2n)}$.
 194 Clearly, these two approaches achieve comparable accuracy if their CIs have the same length. Notably,
 195 confidence interval length alone does not capture the difficulty of evaluation, since the same
 196 interval width may require dramatically different numbers of test samples depending on the underlying
 197 variance. In contrast, ESS can faithfully quantify this difficulty by incorporating the full
 198 predictive distribution, thereby providing a principled measure of the quality and practical value of
 199 scaling prediction. We elaborate this point in Appendix B.

200 We formulate this idea as follows.

201 **Definition 1 (Equivalent Sample Size).** Let \hat{P}_n and \tilde{P} denote the predictive distributions from direct
 202 evaluation and scaling prediction, respectively. Let $\hat{D}_n(\delta)$ and $\tilde{D}(\delta)$ be the minimal lengths of
 203 their $(1 - \delta)$ confidence intervals. We say that \tilde{P} has (n, δ) -equivalent sample size if n satisfies
 204 $\hat{D}_n(\delta) = \tilde{D}(\delta)$. As a special case, we have $\hat{D}_n(\delta) = \sqrt{2 \ln(1/\delta)/n}$ when \hat{P}_n is the empirical
 205 average.

206 The interpretation is straightforward: the scaling prediction achieves the same accuracy as directly
 207 testing the target model on n test points. In what follows, we fix $\delta = 0.05$ and refer to this quantity
 208 simply as the *effective sample size* unless otherwise noted.

209 **Practical Implications of ESS.** ESS provides a principled way to compare scaling prediction with
 210 direct evaluation under a fixed compute budget. A practitioner can either (i) allocate resources to
 211 directly test f^* on n samples, or (ii) evaluate a set of smaller models and fit a scaling law. ESS
 212 quantifies the trade-off: if the ESS exceeds n , scaling prediction delivers higher accuracy per unit
 213 cost. Based on this, the next section further explores how to select the number of models and their

216 sizes to optimally learn the scaling law and improve efficiency. In addition, ESS can be estimated
 217 before any large-scale evaluation, enabling informed decisions in advance.
 218

219 **Connection to Variance of Critical Quantity.** ESS is tightly linked to the uncertainty in predicting
 220 the critical quantity Y . In particular, a smaller variance of Y leads to a larger ESS, as formalized in
 221 Proposition 4.1. This connection highlights that controlling the variance of Y is key to improving
 222 the reliability of scaling predictions. Accordingly, the following sections focus on analyzing and
 223 minimizing $\text{var}(Y)$. [The complete proof of all propositions and theorems throughout the paper are included in Appendix A.](#)

224 **Proposition 4.1.** *When the parameters of Eq. (2) are fixed, ESS increases monotonically as the
 225 variance of the critical quantity Y decreases.*

227 5 EXTRAPOLATION AMPLIFIES PREDICTION UNCERTAINTY

230 We now analyze how extrapolation inflates the variance of scaling predictions and, by Proposi-
 231 tion 4.1, reduces ESS. For the illustration purpose, we use the logarithm of model size as the design
 232 factor X , with X_* corresponding to the target model f^* . Without loss of generality we assume
 233 $X \in [0, \infty)$; otherwise, we can shift and rescale X to ensure non-negative.

234 We introduce the following notations before deriving $\text{var}(Y)$, the key to prediction uncertainty.
 235 Recall the scaling model (1), we denote the variance of the noise ϵ as σ^2 . For M training models,
 236 define sample means $\bar{X}_M := \frac{1}{M} \sum_{i=1}^M X_i$ and the empirical variance $\bar{\sigma}_M^2 := \frac{1}{M} \sum_{i=1}^M (X_i - \bar{X}_M)^2$.

237 **Proposition 5.1** (Variance Characterization of Scaling Prediction). *The variance of the critical
 238 quantity obtained by scaling prediction model (1) is*

$$240 \text{var}(\hat{Y}_*) = \frac{\sigma^2}{M} \cdot \frac{(X_* - \bar{X}_M)^2 + \bar{\sigma}_M^2}{\bar{\sigma}_M^2}. \quad (3)$$

243 Here, the factor σ^2/M reflects the intrinsic random noise in the training data, while $(X_* -$
 244 $\bar{X}_M)^2/\bar{\sigma}_M^2$ captures how far the target model lies outside the training range. In an extrapolation
 245 setting, X_* is typically much larger than \bar{X}_M , so this term dominates the intrinsic noise and
 246 leads to a large variance. In contrast, in classical interpolation where $X_* \leq \max_i X_i$, we have
 247 $(X_* - \bar{X}_M)^2/\bar{\sigma}_M^2 \leq 1$, keeping the variance comparable to the intrinsic noise level. This differ-
 248 ence highlights the inherent instability of scaling predictions, which necessarily extrapolate to larger
 249 models with $X_* > \max_i X_i$.

250 **Example 1.** Suppose a model with one million parameters corresponds to $X = 0$, and X_i 's follow
 251 IID exponential distribution $\text{Exp}(\lambda)$ so that $\mathbb{P}(X_i = x) = \lambda e^{-\lambda x}, x \geq 0$. For a moderate or
 252 large M , we have $\text{var}(\hat{Y}_*) \approx M^{-1} \sigma^2 \{1 + (\lambda X_* - 1)^2\}$, since $\bar{X}_M \approx \mathbb{E}(X) = 1/\lambda$ and $\bar{\sigma}_M^2 \approx$
 253 $\text{var}(X) = 1/\lambda^2$. When $\lambda = 1$, predicting a model of 1,000 billion parameters ($X_* = 6$) yields
 254 $\text{var}(\hat{Y}_*) = 26\sigma^2/M$. In contrast, predicting an in-distribution model ($X_* < \mathbb{E}(X) = 1$) gives at
 255 most $2\sigma^2/M$. Thus, extrapolation inflates the variance roughly by a factor of $(X_* - 1)^2$.

256 Although derived under a linear regression model (1), this variance amplification phenomenon ex-
 257 tends to a broad class of machine learning models, including polynomial regression, k -nearest neigh-
 258 bors, and tree-based methods. These estimators face the same challenge: predicting far beyond the
 259 observed range leaves few, if any, data points near X_* , inevitably increasing the variance of \hat{Y}_* .
 260 In response, the next section develops a theory to find the optimal training design to reduce this
 261 uncertainty and thereby improve the accuracy of scaling predictions.

263 6 UNCERTAINTY REDUCTION BY ACTIVE SELECTION

266 The variance bound in Eq. (3) shows that the distribution of design factors for the small models
 267 largely determines prediction uncertainty. Moreover, Eq. (3) reveals that this variance can be re-
 268 duced by (1) increasing the number of training points M , (2) evaluating models with larger X_i ,
 269 or (3) increasing the spread of the X_i , i.e., increasing their variance. However, evaluating more
 or larger models quickly becomes prohibitively expensive. We therefore propose *active selection*:

270 *optimally allocating the compute budget across both the number and the sizes of the smaller models*
 271 *to minimize prediction variance.*

272 **Objective Function.** Formally, we consider a general problem of predicting the performance of
 273 any target model with design factor $X_* \in [x_l, x_u]$. Let $W(x)$ denote the importance weight for
 274 each target scale x , and $c(x)$ the cost of evaluating a model of size x . Beyond the M existing
 275 models, suppose we can spend a total compute budget C to evaluate k additional models with fac-
 276 tors X_{M+1}, \dots, X_{M+k} . Our goal is to choose k and these new X_{M+j} 's to minimize the following
 277 weighted prediction variance:
 278

$$\begin{aligned} 279 \min_{k \text{ and } X_{M+j}, j=1, \dots, k} & R(k, X_{M+1}, \dots, X_{M+k}; X_1, \dots, X_M, x_l, x_u) \\ 280 & := \int_{[x_l, x_u]} \text{var}(\hat{Y}_*) dW(X_*) \\ 281 & \text{s.t. } \sum_{j=1}^k c(X_{M+j}) \leq C, \quad X_{M+j} \geq 0, j = 1, \dots, k, \\ 282 & \end{aligned} \tag{4}$$

286 where $\text{var}(\hat{Y}_*)$ is the prediction variance given all $M + k$ training points. The special case $x_l = x_u$
 287 recovers the single-target scenario where Eq. (4) reduces to Eq. (3). We also allow $M = 0$, where
 288 no prior evaluations exist and the entire learning trajectory must be designed from scratch. In this
 289 scenario, one selects the sizes of the small models to create the performance scaling law itself, an
 290 idea that motivates the title of our work.

291 **Optimal Solution.** Solving Eq. (4) is highly non-trivial, as it is a non-convex constrained optimiza-
 292 tion problem, a class that is typically NP-hard (Benson, 2006b;a). Interestingly, the objective (4) has
 293 a special structure: it can be expressed as the ratio of two quadratic functions of X_i 's. Exploiting
 294 this structure, we derive a key property of the optimal solution that significantly simplify the optimi-
 295 zation. Specifically, we show that the optimal design turns out to always evaluate at most three
 296 different model scales, though each chosen scale may be sampled multiple times.

297 Before presenting the main result, we introduce a natural assumption. Without loss of generality, let
 298 $X_{M+1} \leq X_{M+2} \leq \dots \leq X_{M+k}$.

300 **Assumption 1.** The cost function $c(x)$ and its second order derivative are non-negative and mono-
 301 tonically increasing, i.e., $c(\alpha) > c(\beta) \geq 0$ and $c''(\alpha) > c''(\beta) \geq 0$ for all $\alpha > \beta \geq 0$.

302 Assumption 1 captures the practical reality that evaluation becomes rapidly more expensive as model
 303 size grows. For example, when x is the logarithm of model size, a cost that grows linearly or
 304 quadratically in size can be written as $c(x) = e^{a+bx}$ for some constants $a \in \mathbb{R}, b > 0$. It can be
 305 verified that Assumption 1 holds for such cost functions.

306 **Theorem 6.1.** *Under Assumption 1, optimal learning of the scaling law under a given computation
 307 budget needs not to use more than two non-zero model scales. Formally, the optimal solution of
 308 Eq. (4) must exhibit one of the following two properties:*

- 310 (1) $0 = X_{M+1}^* = \dots = X_{M+k_1}^* < X_{M+k_1+1}^* = \dots = X_{M+k_2}^* < X_{M+k_2+1}^* \dots = X_{M+k}^*$, and
 311 $\sum_{j=1}^k c(X_{M+k}^*) = C$, where k_1, k_2 are non-negative integers such that $0 \leq k_1 < k_2 < k$; or
 312 (2) $0 = X_{M+1}^* = \dots = X_{M+k_1}^* < X_{M+k_1+1}^* = \dots = X_{M+k}^*$.

314 We illustrate the intuition behind Theorem 6.1 by examining the special case of predicting a sin-
 315 gle target model. In this setting, optimizing (4) reduces to minimizing (3) under a convex budget
 316 constraint. A natural strategy is to fix the number of additional models k and then determine their
 317 optimal sizes. The key step is to “break” the ratio structure in (3) by conditioning on the average
 318 model size \bar{X}_{M+k} . This renders the numerator constant, so the problem reduces to maximizing the
 319 empirical variance. Using variational analysis, we show that any optimal solution contains at most
 320 two non-zero scales; otherwise, reallocating budget from mid-size to larger models would yield a
 321 smaller variance.

322 *Remark 3 (Budget Need Not Be Exhausted).* Theorem 6.1 implies that the budget is fully used only
 323 when the optimal solution involves two nonzero scales. Notably, when the budget is small, it can be
 324 optimal to leave part of it unused. Intuitively, with a small budget it is better to reduce variance by

replicating small models rather than paying for larger ones, so the optimal design may deliberately underspend. For instance, suppose we already have four models of sizes 0.5, 1, 1.5, 2, and a cost function $c(x) = 0.3e^x$. If the budget is $C = 1$, the optimal solution adds three new models of size 0 for a total cost of $0.9 < C$. Increasing the budget to $C = 3$ changes the optimal solution to four models of size 0 plus one medium-scale model of size 1.8.

Implication on Efficient Optimization. Theorem 6.1 not only reveals an interesting property of the optimal solution, but also hints at an efficient polynomial time algorithm for solving the non-convex problem (4) since the characterization of the optimal solution helps drastically reduce the search space. In particular, if the optimal solution only features two model scales, we only need to optimize the single nonzero scale. For an optimal solution with two nonzero scales, the additional constraint $\sum_{j=1}^k c(X_{M+j}^*) = C$ again reduces the problem to a single-variable search. Thus, solving (4) reduces to enumerating all feasible triples $0 \leq k_1 \leq k_2 \leq k \leq C/c(0)$ and optimizing a one-dimensional Lipschitz-continuous objective. Pseudo-code of this procedure is in Appendix C.

How ESS and Active Selection Guide LLM Pre-training Decisions. The ESS characterizes uncertainty in scaling prediction. A small ESS indicates high variance in the predicted results, suggesting that the current scaling curve lacks stability. In such cases, pre-training teams are advised to gather additional data from smaller models before committing to the costly training of a large model. Conversely, a large ESS signifies high confidence in the fitted scaling relationship, enabling teams to make informed decisions about resource investment.

In addition, Theorem 6.1 offers theoretical guidance for proactively planning the architecture and size of future models within an LLM family. Specifically, it establishes the optimal model size allocation strategy that maximizes the ESS under compute constraints, minimizing prediction uncertainty by Proposition 4.1. Theorem 6.1 thus helps pre-training teams design more effective exploration campaigns, accelerating the development of high-performing models with reduced risk.

7 EXPERIMENTS

We evaluate our approach on both simulated and real-world data to show that (1) Equivalent Sample Size (ESS) effectively quantifies and interprets scaling prediction uncertainty, and (2) our active selection algorithm reduces prediction uncertainty under a fixed cost budget, providing practical guidance for optimal experimental design and thus facilitating the learning of performance scaling laws. [Additional experiments and full details are provided in Appendix D](#).

7.1 SIMULATED STUDY

Our first experiment predicts the performance of target models with size $X_* \in (4, 7)$. Following Ruan et al. (2025), we focus on the LLAMA-2 family and its emergent capabilities (Srivastava et al., 2023; Wei et al., 2022) on four tasks: word unscramble, Persian QA, 3-digit subtraction, and 2-digit multiplication.

Data Generation. For illustration, consider the LLAMA-2 family on the word-unscramble task. We take the coefficients of scaling models (1) and (2) from Ruan et al. (2025). The critical quantity and model size (in logarithm) follow $Y = 0.52X - 0.9 + \epsilon$, where ϵ is a standard Gaussian noise with standard deviation equal to 0.2. Model performance P is linked to Y by $P = \sigma(2Y - 6.11)$, where $\sigma(z) = 1/(1 + e^{-z})$ is the standard logistic function. The evaluation cost grows with size as $C(x) = 0.3e^x$.

Methods. We compare two methods, Base and Optimal, in terms of their predicted model performance measured by ESS. Base represents the standard practice of fitting the scaling law in (1) using training models whose sizes are not deliberately chosen (Chen et al., 2024; Ruan et al., 2025; Xu et al., 2025). In our experiment, Base samples $M = 10$ models to fit the scaling law, which are IID from a truncated exponential distribution $truncExp(\lambda = 1, b = 3)$, where b is the upper bound of the truncation.

Subject to the same total evaluation cost as Base, Optimal employs our active selection algorithm to choose model sizes that minimize prediction variance, and thereby maximize ESS. We expect Op-

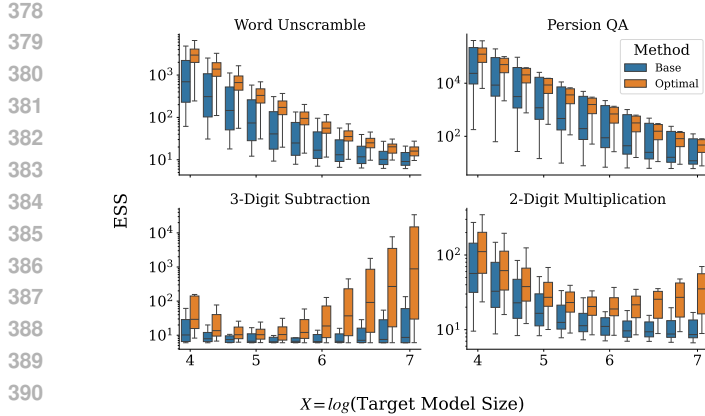


Figure 1: Box-plot of the equivalent sample size (ESS) at varied model size by classic scaling-law-based approach ('Base') and our proposed adaptive selection algorithm ('Optimal') under the same budget. ESS of prediction by models selected by Optimal is significantly higher than that by Base, indicating that Optimal efficiently allocates the budget for maximally improving the reliability of scaling prediction.

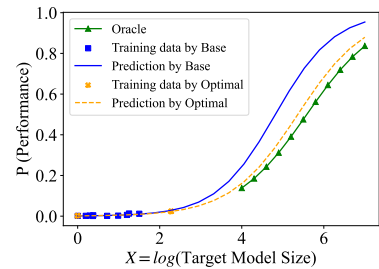


Figure 2: A typical realization of training points and predicted performance curves by classic scaling-law-based approach ('Base') and our proposed adaptive selection algorithm ('Optimal'). 'Oracle' is the true model performance. Optimal stabilizes the curve fit and improves prediction by strategically selecting a few key models that expanding the size range.

timal to achieve substantially higher ESS than Base because it strategically allocates the evaluation budget to reduce the uncertainty inherent in scaling predictions.

Results and Findings. We ran 20 replicates and present a box-plot of ESS versus target model size in Figure 1. The figure shows that Optimal consistently achieves a much higher ESS than Base, especially for large models. For example, in the word unscramble task, the median ESS at $X = 4$ increases from about 500 (Base) to 3000 (Optimal), which is a six-fold gain. It means that the prediction error and uncertainty are significantly reduced by properly selecting training models, aligning with our theoretical findings.

Figure 2, which depicts a typical simulation run, illustrates the reason behind: Base samples mostly small models (blue squares), whereas Optimal strategically selects a few key models (yellow crosses, two around size 2.2 and four near size 0) to expand the size range and stabilize the scaling-law fit.

Moreover, ESS effectively reflects the scaling prediction quality. As shown in Figure 1, ESS remains very low for the 2-Digit Multiplication task, equivalent to only a few dozen test points, indicating that the prediction can be inaccurate and non-confident. We further confirm this implication of ESS by analyzing the prediction error in Appendix D.

7.2 REAL-WORLD APPLICATION: PREDICTING EMERGENT CAPABILITIES

In our simulation studies, the proposed active select algorithm identifies the optimal number and sizes of training models for a given cost budget. In the subsequent real-world experiment, however, model sizes cannot be freely chosen because we cannot access or evaluate new models of arbitrary size. Instead, we must work with the set of models already available to fit the scaling law. Under this constraint, we show that prediction variance can still be reduced, and ESS increased, by applying our active-selection algorithm to choose a subset of the available models that minimizes Eq. (4).

Dataset Collection. We evaluate four emergent LLM capabilities of LLMs: word unscramble, Persian QA, 3-digit subtraction and 2-digit multiplication. We use 72 publicly available models drawn from families such as LLaMA2, Qwen1.5, Falcon, GPT-Neo, OPT, Bloom, and Pythia. Their benchmark performance on datasets including MMLU, HellaSwag, GSM8K, and HumanEval is used to extract the critical quantity Y , following Ruan et al. (2025). We also collect their ground-truth performance on the four emergent tasks and estimate the link function in Eq. (2).

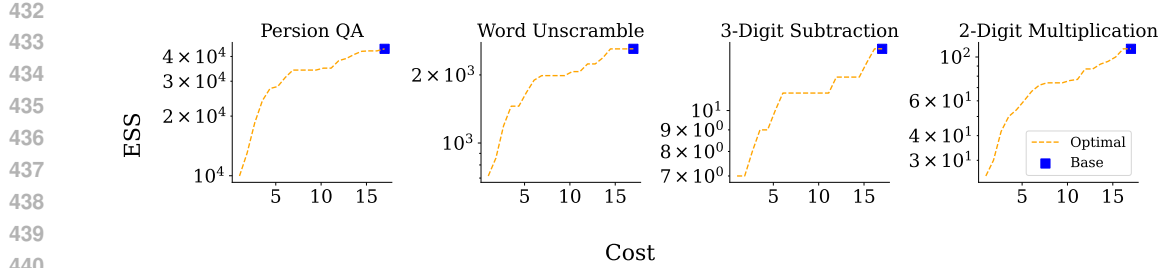


Figure 3: ESS by training on a subset of small OPT models selected by Optimal within a cost budget. Base uses all seven models. Optimal achieves a comparable ESS to Base under a significantly smaller cost.

For the target family, we choose OPT because it offers sufficient models to fit a performance scaling law. Specifically, it has eight models with 125M, 350M, 1.3B, 3B, 7B, 13B, 30B, and 66B parameters. We designate the 66B model as the prediction target, while the remaining seven can be evaluated on the emergent tasks for training. Compute measure X is log-FLOPs calculated as $X = \log(6N \cdot D)$ (Kaplan et al., 2020), where N is the model size and $D = 0.18$ is the pre-training data size. Because all OPT models share the same D , X is linearly correlated with model size. The evaluation cost is $c(x) = 0.3e^x$.

Methods. We compare the ESS of scaling prediction using the same two methods as in the simulation studies: Base and Optimal. In this real-world experiment, Base fits the power law in (1) using all seven smaller OPT models, while Optimal applies our active selection algorithm to choose a cost-constrained subset of available models for fitting the power law. In the experiment, the cost budget of Optimal is varied from 1 to 16.25, where 16.25 is the total cost of evaluating all models. Full details of the scaling-law fitting procedure are provided in Appendix D. We anticipate that Optimal will deliver predictions of accuracy comparable to Base while requiring substantially lower evaluation cost.

Results and Findings. Figure 3 displays the ESS v.s. cost curve for Optimal and the ESS by Base. We have the following key observations from this result. First, Figure 3 demonstrates that a small, well-chosen subset can provide scaling predictions comparable to those obtained from the full set. Across all four tasks, halving the cost budget to $C = 8$ lowers ESS by less than 20%, indicating only a minor loss in predictive power.

Second, we find that four models are consistently selected by our algorithm under a cost budget of $C = 8$: one small model (125M) and three large models (3B, 7B, and 13B). Notably, the total evaluation cost of these models is 6.76, which is below the budget, aligning with our theoretical result that the optimal design need not exhaust the budget.

In Figure 4, we compare the scaling predictions obtained by Base with those derived from the four models selected by Optimal. We report the predicted accuracy, its 95% confidence interval, and the ESS for each method. The result confirms our first observation that the scaling predictions based on Optimal closely match those of Base, while requiring substantially lower cost.

Moreover, the ESS values provide a clear indication of prediction reliability: tasks such as 3-Digit Subtraction and 2-Digit Multiplication exhibit extremely low ESS, signaling that their scaling predictions remain uncertain and may require direct evaluation of the target model or the inclusion of additional smaller models to improve stability.

In summary, these findings underscore that computing the ESS and selecting an appropriate subset allow practitioners to substantially reduce evaluation costs while preserving the reliability of scaling-law predictions; or, equivalently, to enhance reliability without increasing cost.

8 CONCLUSION AND FURTHER REMARKS

Our work introduces Equivalent Sample Size (ESS) as a principled metric for quantifying the uncertainty of scaling-based predictive evaluation of LLMs. By analyzing variance induced by extrapolation, we show that ESS provides a more accurate measure of uncertainty than the standard error of the mean. This work also provides a theoretical foundation for scaling law predictions and a practical method for selecting a subset of models to achieve comparable accuracy at a lower cost.

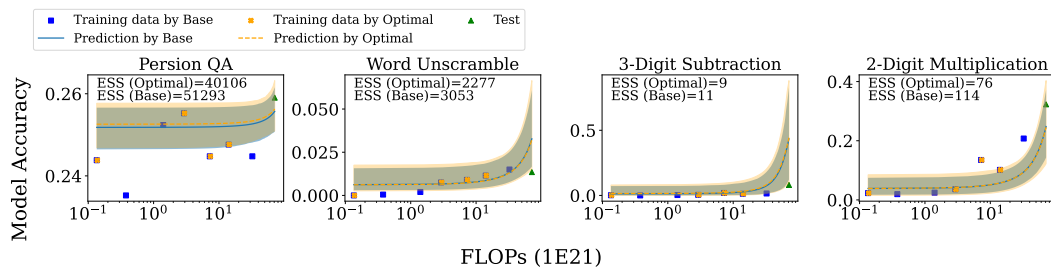


Figure 4: Predicted emergent performance and ESS on the test OPT model. Base uses all seven small OPT models and costs 16.25. Optimal chooses four models to fit the scaling law and costs 6.76. The shaded area is the 95% confidence interval. Optimal achieves nearly the same prediction result and ESS as Base.

lution and proposing an active selection algorithm, we show that practitioners maximize prediction quality by optimally allocating evaluation resources across model sizes.

Despite these contributions, several limitations remain. First, our theoretical analysis assumes that the underlying scaling relationship is correctly specified; if this assumption is violated, predictions may become inaccurate, and the active selection result may be sub-optimal. Developing diagnostics that use ESS to detect model misspecification is therefore a promising direction for future research. Second, our active selection algorithm depends on approximate cost functions and may be sensitive to errors in those estimates, warranting further investigation into how cost-model inaccuracies affect its performance.

REFERENCES

- Ibrahim M Alabdulmohsin, Behnam Neyshabur, and Xiaohua Zhai. Revisiting neural scaling laws in language and vision. *Advances in Neural Information Processing Systems*, 35:22300–22312, 2022.
- Martin Arjovsky, Léon Bottou, Ishaan Gulrajani, and David Lopez-Paz. Invariant risk minimization. *arXiv preprint arXiv:1907.02893*, 2019.
- Yasaman Bahri, Ethan Dyer, Jared Kaplan, Jaehoon Lee, and Utkarsh Sharma. Explaining neural scaling laws. *Proceedings of the National Academy of Sciences*, 121(27):e2311878121, 2024.
- Harold P Benson. Fractional programming with convex quadratic forms and functions. *European Journal of Operational Research*, 173(2):351–369, 2006a.
- Harold P Benson. Maximizing the ratio of two convex functions over a convex set. *Naval Research Logistics (NRL)*, 53(4):309–317, 2006b.
- Xiao Bi, Deli Chen, Guanting Chen, Shanhua Chen, Damai Dai, Chengqi Deng, Honghui Ding, Kai Dong, Qiushi Du, Zhe Fu, et al. Deepseek llm: Scaling open-source language models with longtermism. *arXiv preprint arXiv:2401.02954*, 2024.
- Tom Brown, Benjamin Mann, Nick Ryder, Melanie Subbiah, Jared D Kaplan, Prafulla Dhariwal, Arvind Neelakantan, Pranav Shyam, Girish Sastry, Amanda Askell, et al. Language models are few-shot learners. *Advances in neural information processing systems*, 33:1877–1901, 2020.
- Ethan Caballero, Kshitij Gupta, Irina Rish, and David Krueger. Broken neural scaling laws. *arXiv preprint arXiv:2210.14891*, 2022.
- Yangyi Chen, Binxuan Huang, Yifan Gao, Zhengyang Wang, Jingfeng Yang, and Heng Ji. Scaling laws for predicting downstream performance in llms. *Transaction of Machine Learning Research*, 2024.
- Leshe Choshen, Yang Zhang, and Jacob Andreas. A hitchhiker’s guide to scaling law estimation. *arXiv preprint arXiv:2410.11840*, 2024.

- 540 Corinna Cortes, Lawrence D Jackel, Sara Solla, Vladimir Vapnik, and John Denker. Learning
 541 curves: Asymptotic values and rate of convergence. *Advances in neural information processing*
 542 *systems*, 6, 1993.
- 543
- 544 Zhengxiao Du, Aohan Zeng, Yuxiao Dong, and Jie Tang. Understanding emergent abilities of
 545 language models from the loss perspective. *Advances in neural information processing systems*,
 546 37:53138–53167, 2024.
- 547 Samir Yitzhak Gadre, Georgios Smyrnis, Vaishaal Shankar, Suchin Gururangan, Mitchell Worts-
 548 man, Rulin Shao, Jean Mercat, Alex Fang, Jeffrey Li, Sedrick Keh, et al. Language models scale
 549 reliably with over-training and on downstream tasks. *arXiv preprint arXiv:2403.08540*, 2024.
- 550
- 551 Alex Hägele, Elie Bakouch, Atli Kosson, Leandro Von Werra, Martin Jaggi, et al. Scaling laws
 552 and compute-optimal training beyond fixed training durations. *Advances in Neural Information
 553 Processing Systems*, 37:76232–76264, 2024.
- 554
- 555 Dan Hendrycks, Steven Basart, Norman Mu, Saurav Kadavath, Frank Wang, Evan Dorundo, Rahul
 556 Desai, Tyler Zhu, Samyak Parajuli, Mike Guo, et al. The many faces of robustness: A criti-
 557 cal analysis of out-of-distribution generalization. In *Proceedings of the IEEE/CVF international
 558 conference on computer vision*, pp. 8340–8349, 2021.
- 559
- 560 Wassily Hoeffding. Probability inequalities for sums of bounded random variables. *Journal of the
 561 American statistical association*, 58(301):13–30, 1963.
- 562
- 563 Jordan Hoffmann, Sebastian Borgeaud, Arthur Mensch, Elena Buchatskaya, Trevor Cai, Eliza
 564 Rutherford, Diego de las Casas, Lisa Anne Hendricks, Johannes Welbl, Aidan Clark, Tom Henni-
 565 gan, Eric Noland, Katherine Millican, George van den Driessche, Bogdan Damoc, Aurelia Guy,
 566 Simon Osindero, Karen Simonyan, Erich Elsen, Oriol Vinyals, Jack William Rae, and Laurent
 567 Sifre. An empirical analysis of compute-optimal large language model training. In *Advances in
 568 Neural Information Processing Systems*, 2022.
- 569
- 570 Thomas Hofmann, Bernhard Schölkopf, and Alexander J Smola. Kernel methods in machine learn-
 571 ing. *Annals of Statistics*, 2008.
- 572
- 573 Jared Kaplan, Sam McCandlish, Tom Henighan, Tom B. Brown, Benjamin Chess, Rewon Child,
 574 Scott Gray, Alec Radford, Jeff Wu, and Dario Amodei. Scaling laws for neural language
 575 models. *ArXiv*, abs/2001.08361, 2020. URL <https://api.semanticscholar.org/CorpusID:210861095>.
- 576
- 577 Da Li, Yongxin Yang, Yi-Zhe Song, and Timothy Hospedales. Learning to generalize: Meta-learning
 578 for domain generalization. In *Proceedings of the AAAI conference on artificial intelligence*, vol-
 579 ume 32, 2018.
- 580
- 581 Jiashuo Liu, Zheyuan Shen, Yue He, Xingxuan Zhang, Renzhe Xu, Han Yu, and Peng Cui. Towards
 582 out-of-distribution generalization: A survey. *arXiv preprint arXiv:2108.13624*, 2021.
- 583
- 584 David Owen. How predictable is language model benchmark performance? *arXiv preprint
 585 arXiv:2401.04757*, 2024.
- 586
- 587 Jonas Peters, Peter Bühlmann, and Nicolai Meinshausen. Causal inference by using invariant pre-
 588 diction: identification and confidence intervals. *Journal of the Royal Statistical Society Series B:
 589 Statistical Methodology*, 78(5):947–1012, 2016.
- 590
- 591 Felipe Maia Polo, Seamus Somerstep, Leshem Choshen, Yuekai Sun, and Mikhail Yurochkin. Sloth:
 592 scaling laws for llm skills to predict multi-benchmark performance across families. *arXiv preprint
 593 arXiv:2412.06540*, 2024.
- 594
- 595 Jonathan S Rosenfeld, Amir Rosenfeld, Yonatan Belinkov, and Nir Shavit. A constructive prediction
 596 of the generalization error across scales. *arXiv preprint arXiv:1909.12673*, 2019.
- 597
- 598 Yangjun Ruan, Chris J Maddison, and Tatsunori B Hashimoto. Observational scaling laws and
 599 the predictability of language model performance. *Advances in Neural Information Processing
 600 Systems*, 37:15841–15892, 2025.

- 594 Aarohi Srivastava, Abhinav Rastogi, Abhishek Rao, Abu Awal Shoeb, Abubakar Abid, Adam Fisch,
 595 Adam R Brown, Adam Santoro, Aditya Gupta, Adri Garriga-Alonso, et al. Beyond the imitation
 596 game: Quantifying and extrapolating the capabilities of language models. *Transactions on*
 597 *machine learning research*, 2023.
- 598 Hugo Touvron, Louis Martin, Kevin Stone, Peter Albert, Amjad Almahairi, Yasmine Babaei, Niko-
 599 lay Bashlykov, Soumya Batra, Prajjwal Bhargava, Shruti Bhosale, et al. Llama 2: Open founda-
 600 tion and fine-tuned chat models. *arXiv preprint arXiv:2307.09288*, 2023.
- 601 Jason Wei, Yi Tay, Rishi Bommasani, Colin Raffel, Barret Zoph, Sebastian Borgeaud, Dani Yo-
 602 gatama, Maarten Bosma, Denny Zhou, Donald Metzler, et al. Emergent abilities of large language
 603 models. *Transactions on machine learning research*, 2022.
- 604 Chuhuan Wu and Ruiming Tang. Performance law of large language models. *arXiv preprint*
 605 *arXiv:2408.09895*, 2024.
- 606 Chengyin Xu, Kaiyuan Chen, Xiao Li, Ke Shen, and Chenggang Li. Unveiling downstream per-
 607 formance scaling of llms: A clustering-based perspective. *arXiv preprint arXiv:2502.17262*, 2025.
- 608 Haotian Ye, Chuanlong Xie, Tianle Cai, Ruichen Li, Zhenguo Li, and Liwei Wang. Towards a
 609 theoretical framework of out-of-distribution generalization. *Advances in Neural Information Pro-
 610 cessing Systems*, 34:23519–23531, 2021.
- 611 Qinyuan Ye, Harvey Yiyun Fu, Xiang Ren, and Robin Jia. How predictable are large language
 612 model capabilities? a case study on big-bench. *arXiv preprint arXiv:2305.14947*, 2023.
- 613 Xiaohua Zhai, Alexander Kolesnikov, Neil Houlsby, and Lucas Beyer. Scaling vision transformers.
 614 In *Proceedings of the IEEE/CVF conference on computer vision and pattern recognition*, pp.
 615 12104–12113, 2022.
- 616 Qiyuan Zhang, Fuyuan Lyu, Xue Liu, and Chen Ma. Collaborative performance prediction for large
 617 language models. *arXiv preprint arXiv:2407.01300*, 2024.
- 618 Han Zhao, Remi Tachet Des Combes, Kun Zhang, and Geoffrey Gordon. On learning invariant
 619 representations for domain adaptation. In *International conference on machine learning*, pp.
 620 7523–7532. PMLR, 2019.
- 621
- 622
- 623
- 624
- 625
- 626
- 627
- 628
- 629
- 630
- 631
- 632
- 633
- 634
- 635
- 636
- 637
- 638
- 639
- 640
- 641
- 642
- 643
- 644
- 645
- 646
- 647

648 A MISSING PROOFS
649650 **Proof of Proposition 4.1.**
651653 *Proof.* When ω and b are fixed, any $(1 - \delta)$ -CI of Y , denoted by $[Y_l, Y_u]$, induces a corresponding
654 $(1 - \delta)$ -CI of P , given by $[P_l, P_u]$ where $P_l = \sigma(\omega Y_l + b)$ and $P_u = \sigma(\omega Y_u + b)$. Since the predicted
655 Y is Gaussian, a smaller variance of Y yields a tighter interval $|Y_u - Y_l|$. By the monotonicity of
656 $\sigma(\cdot)$, this translates to a narrower confidence interval $[P_l, P_u]$. According to the definition of ESS,
657 a smaller confidence interval corresponds to a larger ESS, as it reflects the number of test samples
658 needed to achieve the same level of precision through direct evaluation. \square
659660 **Proof of Proposition 5.1**
661663 *Proof.* We define \bar{Y}_M and \bar{XY}_M , and $\bar{X^2}_M$ analogously to \bar{X}_M . By classic learning theory, the
664 least-squares estimates of coefficients in Eq. (1) are
665

666
$$\hat{\alpha}_M = \bar{Y}_M - \hat{\beta}_M \bar{X}_M, \quad \hat{\beta}_M = \frac{\bar{XY}_M - \bar{X}_M \bar{Y}_M}{\bar{X^2}_M - \bar{X}_M^2}.$$

667
668

669 Therefore, the predicted critical quantity at X_* is $\hat{Y}_* = \hat{\alpha}_M + \hat{\beta}_M X_*$, whose variance is
670

671
$$\text{var}(\hat{Y}_*) = \mathbb{E}(\hat{\alpha}_M + \hat{\beta}_M X_* - \alpha + \beta X_*)^2 = \frac{\sigma^2}{M} \cdot \frac{(X_* - \bar{X}_M)^2 + \bar{\sigma}_M^2}{\bar{\sigma}_M^2}.$$

672
673

674 \square
675
676677 **Proof of Theorem 6.1.**
678679 *Proof.* The original optimization problem can be rewritten as
680

681
$$\begin{aligned} \min_{k \text{ and } X_{M+j}, j=1, \dots, k} & R(k, X_{M+1}, \dots, X_{M+k}; X_1, \dots, X_M, x_l, x_u) \\ & := \int_{[x_l, x_u]} \frac{\sigma^2}{M+k} \cdot \frac{(x - \bar{X}_{M+k})^2 + \bar{\sigma}_{M+k}^2}{\bar{\sigma}_{M+k}^2} dW(x) \\ & = \frac{\sigma^2}{(M+k)\bar{\sigma}_{M+k}^2} \cdot [\{\bar{X}_{M+k} - \mathbb{E}_W(X_*)\}^2 + \text{var}_W(X_*) + \bar{\sigma}_{M+k}^2], \quad (5) \\ & \text{s.t. } \sum_{j=1}^k c(X_{M+j}) \leq C, \\ & X_{M+j} \geq 0, j = 1, \dots, k. \end{aligned}$$

693 where $\mathbb{E}_W(X_*) = \int_{[x_l, x_u]} x dW(x)$ and $\text{var}_W(X_*) = \int_{[x_l, x_u]} (x - \mathbb{E}_W(X))^2 dW(x)$.
694695 We first show that the optimal design contains at most three different scales.
696697 **Step 1: Conditioning.** We denote $z_j := X_{M+j}, j = 1, \dots, k$. For any fixed k , let $z_j^*, j = 1, \dots, k$
698 be any optimal solution and $Z^* = \sum_{i=1}^k z_j^*$ be their sum. Consider a variant of Optimization Prob-
699 lem (1) – more specifically, a simplified version – in which both k and Z^* values are pre-given and
700 fixed; hence the goal is simplified to identify the optimal $z_1^*, z_2^*, \dots, z_k^*$ that minimizes the objec-
701 tive of (1) subject to given condition $\sum_{i=1}^k z_j = Z^*$. The advantage of considering this simplified
version is that the enumerator now becomes a constant, hence the objective is now equivalent to

702 maximize its denominator. Specifically, given a fixed k and Z^* , we have
 703

$$\begin{aligned}
 704 \quad & \min_{k; X_{M+1}, \dots, X_{M+k}} R(k, X_{M+1}, \dots, X_{M+k}; X_1, \dots, X_M, x_l, x_u) \\
 705 \quad & \Leftrightarrow \min_{z_j, j=1, \dots, k: \sum z_j = Z^*} \frac{\sigma^2}{(M+k)\bar{\sigma}_{M+k}^2} \cdot [\{\bar{X}_{M+k} - \mathbb{E}_W(X_*)\}^2 + \text{var}_W(X_*) + \bar{\sigma}_{M+k}^2] \\
 706 \quad & \Leftrightarrow \min_{z_j, j=1, \dots, k: \sum z_j = Z^*} \frac{1}{\bar{\sigma}_{M+k}^2} \Leftrightarrow \max_{z_j, j=1, \dots, k: \sum z_j = Z^*} \bar{\sigma}_{M+k}^2 \\
 707 \quad & \Leftrightarrow \max_{z_j, j=1, \dots, k: \sum z_j = Z^*} \sum_{i=1}^M (X_i - \bar{X}_{M+k})^2 + \sum_{j=1}^k (z_j - \bar{X}_{M+k})^2 \\
 708 \quad & \Leftrightarrow \max_{z_j, j=1, \dots, k: \sum z_j = Z^*} \sum_{j=1}^k z_j^2,
 \end{aligned}$$

709 since $\bar{X}_{M+k} = (\sum_{i=1}^M X_i + \sum_{j=1}^k z_j)/(M+k)$ is a constant.
 710

711 As a result, optimizing (5) is equivalent to maximizing the variance of additional points z_j 's. The
 712 argument above leads to the following re-formulation of OP (5), by conditioning it on the constraint
 713 $Z^* = \sum_{j=1}^k z_i^*$:

$$\begin{aligned}
 714 \quad & \max_{k \text{ and } z_1, \dots, z_k} \sum_{i=1}^k z_i^2 \\
 715 \quad & \text{subject to} \quad \sum_{i=1}^k c(z_i) \leq C, \\
 716 \quad & \quad \sum_{i=1}^k z_i = Z^*, \\
 717 \quad & \quad z_i \geq 0, \forall i = 1, \dots, k.
 \end{aligned} \tag{6}$$

718 Notably, despite its simplification, OP (6) is still challenging to solve because its objective is to
 719 maximize a convex function which generally is NP-hard. Nevertheless, we show that for any given
 720 Z^* and any k value, any optimal solution to OP (6) must be able to be expressed as $z_1^* = z_2^* = \dots =$
 721 $z_{k_1}^* = 0$, $z_{k_1+1}^* = z_{k_1+2}^* = \dots = z_{k_2}^* = \alpha$ and $z_{k_2+1}^* = z_{k_2+2}^* = \dots = z_k^* = \beta$ for some $0 < \alpha < \beta$ and
 722 $0 \leq k_1 \leq k_2 \leq k$.

723 **Step 2: Proving by contradiction.** Suppose the claim above is not true, then there must exist three
 724 non-zero z_i^* 's with varied values. Without loss of generality, let these three variables be $0 < z_1^* <$
 725 $z_2^* < z_3^*$. Next we argue that, in such cases, there must exist a way to strictly increase the objective
 726 value without violating the constraints, hence contradicting their optimality.

727 Our argument employs the variational methods. Consider new variables $z_1 = z_1^* - \epsilon_1$, $z_2 = z_2^* + \epsilon_2$
 728 and $z_3 = z_3^* - \epsilon_3$ for some arbitrarily small $\epsilon_1, \epsilon_2, \epsilon_3 > 0$ such that

$$-c'(z_1^*)\epsilon_1 + c'(z_2^*)\epsilon_2 - c'(z_3^*)\epsilon_3 = 0 \tag{7}$$

$$-\epsilon_1 + \epsilon_2 - \epsilon_3 = 0 \tag{8}$$

729 Specifically, these two constraints ensures that the new variables z_1, z_2, z_3 remain feasible for OP
 730 (6) when $\epsilon_1, \epsilon_2, \epsilon_3$ are arbitrarily small since their relations expressed above guarantee the variation
 731 between z_1, z_2, z_3 and z_1^*, z_2^*, z_3^* to be 0 for all constraints. However, we argue that the variation of
 732 the objective of OP (6) between z_1, z_2, z_3 and z_1^*, z_2^*, z_3^* is strictly positive, i.e., z_1, z_2, z_3 achieves
 733 higher/better objective. Equality (8) implies $\epsilon_2 = \epsilon_1 + \epsilon_3$. Substituting ϵ_2 in Equality (7), we obtain

$$\epsilon_1[c'(z_2^*) - c'(z_1^*)] = \epsilon_3[c'(z_3^*) - c'(z_2^*)]$$

734 The mean value theorem implies that there exists $u_1 < u_2$ such that $\epsilon_1 c''(u_1)[z_2^* - z_1^*] =$
 735 $\epsilon_3 c''(u_2)[z_3^* - z_2^*]$ By our assumption, all terms are positive and $0 \leq c''(u_1) < c''(u_2)$, hence
 736 we must have

$$\epsilon_1[z_2^* - z_1^*] > \epsilon_3[z_3^* - z_2^*].$$

756 This implies the variation of the objective under z_1, z_2, z_3 and z_1^*, z_2^*, z_3^* is strictly positive, i.e.,
 757

$$\begin{aligned}\Delta &= -2z_1^*\epsilon_1 + 2z_2^*\epsilon_2 - 2z_3^*\epsilon_3 \\ &= -2z_1^*\epsilon_1 + 2z_2^*(\epsilon_1 + \epsilon_3) - 2z_3^*\epsilon_3 \\ &= 2[z_2^* - z_1^*]\epsilon_1 - 2[z_3^* - z_2^*]\epsilon_3 \\ &> 0.\end{aligned}$$

762 This contradicts the optimality of z_1^*, z_2^*, z_3^* , as desired.
 763

764 Next, we show that the optimal design must satisfy $\sum_{j=1}^k c(z_j) = C$ when there are three scales,
 765 namely when $k_1 < k_2 < k$. We prove by constructing a contradiction. Suppose $z_j^*, j = 1, \dots, k$ is
 766 an optimal design of OP (6) such that $\sum_{j=1}^k c(z_j^*) < C$ and there are three different scales. WLOG,
 767 we can let $0 = z_1^* < z_2^* < z_3^*$. Now, let $z_2 = z_2^* - \epsilon$, $z_3 = z_3^* + \epsilon$, and $z_j = z_j^*$ for $j \neq 2, 3$, where
 768 ϵ is a positive constant. Since $\sum_{j=1}^k c(z_j^*) < C$, there exists a sufficiently small ϵ such that z_i 's is a
 769 valid solution to OP (6). However, the corresponding objective is
 770

$$\sum_{j=1}^k z_j^2 = \sum_{j=1}^k (z_j^*)^2 + 2\epsilon(z_3^* - z_2^*) + 2\epsilon^2 > \sum_{j=1}^k (z_j^*)^2,$$

774 which is a contradiction. We thus completes the proof. \square
 775

776 B EXTENSIONS OF ESS

777 The ESS definition is not tied to Hoeffding-based confidence intervals. Rather, ESS can leverage the
 778 *entire predictive distribution* produced by scaling prediction. The Hoeffding bound is distribution-
 779 free and conservative, as it does not exploit properties of f^* . In this section, we discuss a Bayesian
 780 formulation that can yield tighter ESS estimates.
 781

782 We use zero-one loss as the loss function for the illustration purpose. For direct evaluation, we
 783 construct the distribution of \hat{P}_n through a Bayesian approach. In particular, we assign a uniform
 784 distribution as \hat{P}_0 , which serves as a non-information prior distribution. After evaluating each test
 785 point, we update the posterior distribution \hat{P}_n by the Bayesian theorem. As a result, the posterior
 786 distribution will follow a Beta distribution $Beta(\alpha, \beta)$, where α and β can be interpreted as the
 787 number of zeros and ones in the evaluation results, respectively. We can therefore match the distribution
 788 of \hat{P} and $Beta(\alpha, \beta)$ as follows. Let $m_1 = \mathbb{E}(\hat{P})$ and $m_2 = \text{var}(\hat{P})$. We can solve α and β
 789 from the following moment equations:
 790

$$\begin{aligned}m_1 &= \alpha/(\alpha + \beta), \\ m_2 &= \frac{\alpha\beta}{(\alpha + \beta)^2(\alpha + \beta + 1)}.\end{aligned}$$

794 In particular, we have the close-form solution
 795

$$\begin{aligned}\alpha &= m_1[\{m_1(1 - m_1)\}/m_2 - 1], \\ \beta &= (1 - m_1)[\{m_1(1 - m_1)\}/m_2 - 1].\end{aligned}$$

796 Consequently, the scaling prediction has an ESS equals \tilde{n} , where $\tilde{n} := \alpha + \beta = \{m_1(1 - m_1)\}/m_2 - 1$. We note that \tilde{n} is guaranteed to be non-negative as $m_2 = \text{var}(\hat{P}) = \mathbb{E}(\hat{P}^2) - \{\mathbb{E}(\hat{P})\}^2 \leq 800 m_1 - (m_1)^2$, where the last step is due to $P \in [0, 1]$.
 801

802 To illustrate the benefit of ESS, consider a model family with very poor accuracy. In this case,
 803 direct evaluation requires only a small number of test samples: the observed outputs are consis-
 804 tently incorrect, the empirical variance is low, and the confidence interval quickly becomes narrow.
 805 Scaling prediction reflects this by producing a predictive distribution highly concentrated near low
 806 performance, which leads to a **small ESS**, thereby accurately capturing the low evaluation cost
 807 needed in practice.
 808

809 Now consider a model family with moderate accuracy (e.g., 50%). Direct evaluation requires many
 810 more samples to obtain a confidence interval of the same width. In this scenario, ESS appropriately
 811 increases, reflecting the greater sample size needed to reliably estimate performance.
 812

810 In summary, ESS can faithfully quantify the evaluation difficulty by incorporating the full predictive
 811 distribution, thereby providing a principled measure of the quality and practical value of scaling
 812 prediction.

814 C PSEUDO-CODE OF THE ACTIVE SELECTION ALGORITHM

817 The active selection algorithm for solving (4) is summarized in Algorithm 1, with Algorithm 2
 818 serving as a subroutine that computes the optimal solution for each fixed pair (k_1, k_2) .

820 **Algorithm 1** Active Selection

821 **Require:** The budget C , cost function $c(\cdot)$, and target region $[x_l, x_u]$
 822 1: **for** $k = 1, 2, \dots$ **do**
 823 2: Let $R_k, X_1, \dots, X_k \leftarrow \text{BestDesign}(k)$
 824 3: Stop if the smallest cost of evaluating k models exceeds C
 825 4: **end for**
 826 5: Return the design with the smallest R_k
 827 **Output:** The optimal design X_1, \dots, X_k .

830 **Algorithm 2** Best Design with a Fixed Number of Models

831 **Require:** The budget C , cost function $c(\cdot)$, number of points k , and target region $[x_l, x_u]$ and its
 832 distribution W .
 833 1: **for** $0 \leq k_1 \leq k_2 \leq k$ **do**
 834 2: Let $X_1, \dots, X_{k_1} = 0, X_{k_2+1}, \dots, X_k = x$
 835 3: Let $X_{k_1+1}, \dots, X_{k_2} = v$, where v is determined by $\sum_{j=1}^k c(X_j) = C$.
 836 4: Solve x that minimizes Eq. (4), and let R_{k_1, k_2} be the minimum
 837 5: **end for**
 838 6: Return the design with the smallest R_{k_1, k_2}
 839 **Output:** The optimal design X_1, \dots, X_k .

843 D EXPERIMENT DETAILS AND ADDITIONAL RESULTS.

844 D.1 SCALING PREDICTION WITH REAL WORLD DATASET

845 For the Base method, we follow the procedure described in (Ruan et al., 2025). First, we fit the link
 846 function in Eq. (2) using the performance of all models **excluding** the target family (LLaMA2) on
 847 the emergent benchmark. The link function is specified as

$$851 \sigma(x) = h + (1 - h)/(1 + e^{-\omega Y - b}),$$

853 where $h \in [0, 1]$ and $\omega, b \in \mathbb{R}$ are coefficients.

854 Next, we fit the scaling law in Eq. (1) using the training OPT models. The critical quantity Y for
 855 each model is extracted by applying PCA to the imputed performance matrix B . Here, each entry
 856 of B is the standardized performance of a training model on a benchmark such as MMLU. The
 857 final predicted performance is obtained by plugging the extrapolated critical quantity Y of the target
 858 model into Eq. (2).

859 For Optimal, all steps remain the same except that only a subset of OPT models selected by our
 860 active selection algorithm (along with models from other families) are included in the training set.

861
 862 The $(1 - \delta)$ -confidence interval (CI) is constructed as follows. We first compute a $(1 - \delta/2)$ -CI for
 863 \hat{Y} using Eq. (3). Then, we obtain a $(1 - \delta/2)$ -CI for the link function (2) via bootstrapping. Finally,
 864 we combine these results through a plug-in procedure to produce the overall $(1 - \delta)$ -CI.

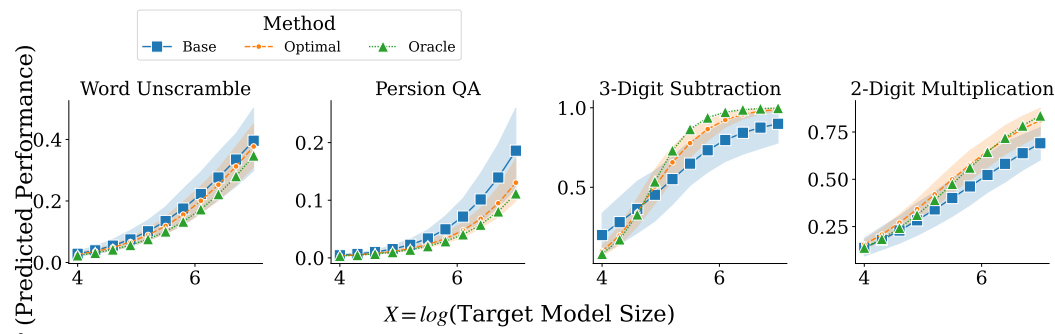


Figure 5: Predicted model performance at varied model size by classic scaling-law-based approach ('Base') and our proposed adaptive selection algorithm ('Optimal'). The true model performance is denoted as 'Oracle'.

D.2 SIMULATED STUDIES

In addition to ESS, we report the predicted performance of both Base and Optimal in Figure 5. The figure shows that Optimal achieves both lower prediction error and smaller variance than Base, mirroring the ESS improvements observed in Figure 1. This consistency reinforces that ESS reliably captures the quality of scaling predictions and serves as an intuitive measure of their reliability.

E RELAXATION OF TECHNICAL ASSUMPTIONS

While our theoretical analysis is built on simplified assumptions to derive clean results, the underlying ideas and optimization pipeline of our framework are general and can be extended to more complex and practical scenarios. Below, we outline several promising directions for such generalizations.

E.1 RELAXATION OF THE LINEAR MODEL ASSUMPTION

The simple linear model in Eq. (1) serves as a starting point, but our framework is not limited to this form:

- **Multi-variable linear regression.** By allowing a multi-variate input X , the model can naturally incorporate multiple explanatory factors, such as model size, training dataset size, learning rate, and other architectural or training hyperparameters.
- **Interaction effects.** Cross-factor terms (e.g., the product of model size and dataset size) can be included in X to capture interaction effects, enabling richer modeling while retaining linearity in parameter space.
- **Nonlinear feature expansion.** Using the kernel trick Hofmann et al. (2008), especially polynomial kernels, we can effectively work in high- or infinite-dimensional feature spaces that include all polynomial combinations of base factors.
- **Approximate linearity.** Many real-world relationships are well approximated by polynomial or piecewise linear functions, making linear modeling a reasonable and practical simplification in many cases.

Model mis-specification. In scenarios where the true relationship deviates significantly from our assumed linear form, the predictions may become biased. While this challenge is inherent to all model-based prediction, our framework provides a safeguard: the Equivalent Sample Size (ESS) can be computed on training points to assess the reliability of the model (e.g., using cross validation). A large discrepancy may indicate model misspecification, and how to adaptively refine the model based on such feedback is a promising direction for future work.

918 E.2 RELAXATION OF THE NOISE DISTRIBUTION ASSUMPTION
919920 Our analysis assumes Gaussian noise primarily for technical convenience. However, the prediction
921 variance in Eq. (3) remains valid under broader settings as long as the noise has bounded variance,
922 which is a standard assumption in learning theory. This implies that the core optimization ob-
923 jective (4) remains largely unaffected. Nevertheless, constructing valid confidence intervals under
924 non-Gaussian noise requires calibration, which can be addressed through methods such as bootstrap
925 resampling or empirical estimation based on the residuals.926 E.3 RELAXATION OF THE LINK FUNCTION ASSUMPTION
927928 We allow the link function $\sigma(\cdot)$ in Eq. (2) to be an arbitrary and possibly unknown function. When
929 $\sigma(\cdot)$ is unknown, non-parametric regression methods such as kernel smoothing or k -nearest neigh-
930 bors can be used to estimate $\sigma(\cdot)$ from the training data. Bootstrapping techniques can then be
931 used to construct prediction intervals, allowing our framework to remain statistically grounded even
932 without strong assumptions on the link function.934 F THE USE OF LARGE LANGUAGE MODELS STATEMENT
935936 Large language models were used solely as a writing aid. Their use was limited to minor language
937 editing, such as correcting grammar, improving clarity, and polishing the phrasing, without altering
938 the substantive content or analysis of the article.